# Towards Large-Scale RFID Positioning: A Low-cost, High-precision Solution Based on Compressive Sensing

†Liqiong Chang, †Xinyi li, †Ju Wang, ‡Haining Meng, †Xiaojiang Chen*
†Dingyi Fang, †Zhanyong Tang, §Zheng Wang
†Northwest University, ‡Chinese Academy of Sciences, §Lancaster University

***Abstract*—RFID-based positioning is emerging as a promising solution for inventory management in places like warehouses and libraries. However, existing solutions either are too sensitive to the environmental noise, or require deploying a large number of reference tags which incur expensive deployment cost and increase the chance of data collisions. This paper presents CSRP, a novel RFID based positioning system, which is highly accurate and robust to environmental noise, but relies on much less reference tags compared with the state-of-the-art. CSRP achieves this by employing an noise-resilient RFID fingerprint scheme and a compressive sensing based algorithm that can recover the target tag's position using a small number of signal measurements. This work provides a set of new analysis, algorithms and heuristics to guide the deployment of reference tags and to optimize the computational overhead. We evaluate CSRP in a deployment site with 270 commercial RFID tags. Experimental results show that CSRP can correctly identify 84.7% of the test items, achieving an accuracy that is comparable to the state-of-the-art, using an order of magnitude less reference tags.**

## I. INTRODUCTION

Radio Frequency IDentificaiton (RFID) is rapidly emerging as a viable means for tracking and localizing objects [1]–[6]. By simply attaching tags to objects, one can then identify the ID of an object of interest and locate its position – by using an contactless RFID reader to gather data from object tags based on a pre-defined radio frequency and protocol. RFID-based positioning is widely seen as a promising solution for inventory management in places like warehouses and libraries [7].

Prior work in RFID-based positioning systems exploits the received signal strength (RSS) information of surrounding object tags to estimate the target's location [1]–[4]. However, such an approach is unreliable as the RSS reading is inherently sensitive to the environmental noise. As an alternative, the Angel of Arrival (AOA) approach [8]–[10] employs multiple antennas to cancel the environmental noise. An AOA scheme calculates the target object's location by measuring the differences of the radio frequency (RF) signal phases between the target tags and antennas. The working mechanism of AOA assumes that the RF signal travels in a direct, line-of-sight (LOS) path from the source to the receiver. This assumption means that the positioning precision can be greatly affected by any physical object that obstructs the signal transmission path – a problem known as non-line-of-sight (NLOS) propagation.

PinIt is the current state-of-the-art RFID-based positioning system [6]. It was proposed to address the NLOS issue. PinIt works by first deploying reference tags at known locations, and then using a reference tag that has the most similar signal characteristics to the target tag to estimate the target's position. To achieve a high accuracy, PinIt requires placing a large number of reference tags, sometimes having more reference tags than the deployed ones. This large number of reference tags not only incurs high deployment cost, but also increases the chance of data collisions between tags and leads to deleterious performance in a large-scale deployment. To make RFID-based positioning practical at scale, we must cut down the number of reference tags required.

This paper introduces CSRP, a novel RFID positioning system that works with NLOS. One of the advantages of CSRP is that it requires significantly less reference tags than the state-of-the-art but without scarifying the precision. Our key insight is that the number of tags to be positioned at a given moment in a large-scale deployment is highly likely to be smaller than the total number of tags. If we consider the problem of positioning as finding a location vector where an element with a value of '1' marks a target tag of a specific location and '0' otherwise, then most of the elements of the vector will be zero, i.e., the location vector is sparse. The sparsity of the location vector suggests that through optimization, it is possible to recover the sparse location vector by sampling a small number of reference tags – using a recently established signal processing technique called compressive sensing (CS) [11]. Essentially, CS allows one to reconstruct a sparse signal (i.e., the location vector in our case) from far fewer samples (i.e., reference tags in our case) than required by the Shannon-Nyquist sampling theorem under certain conditions [12]. If this can be achieved, we can then greatly reduce the number of reference tags required; and consequently, we can save cost and time, and decrease the chance of data collision in a large-scale RFID deployment.

Transforming this high-level idea into a practical system is non-trivial, because we have to rely on a small number of reference tags. It is undesirable to use the signal measurement of a deployed target tag as the fingerprint for positioning like prior work [1], [4]. This is because an instantaneous measurement for a tag can significantly differ from the previous measurement of the same tag due to the dynamic environmental

noise. We cannot use the signal multipath profiles of nearby reference tags to estimate the location of a deployed target tag like PinIt does either. This is because our small number of reference tags will have to be sparsely distributed in the deployment site and as a result, many object tags will be far from a reference tag.

Our solution is to calculate, for a deployed object tag, its spatial relation with respect to each reference tag in terms of their multipath profiles. We then use this relation to build a fingertip matrix (or database) for all object tags. The key of our approach is to use the relatively stable spatial relation between an object tag and those static, fixed reference tags to reduce or even cancel the dynamic environmental noise. Since the spatial relation is automatically calculated, the fingertip matrix will be updated if any of the object tags has been replaced or moved. This ability allows CSRP to adapt to the changing deployment environment without human involvement.

To locate a target tag, we first use an RFID reader to measure the multipath profile of that tag. Next, we calculate the spatial relation between the multipath profiles of the target tag and each static reference tag. We organize the calculated spatial relations as an one-dimensional vector of real values, for which we called a ***real-time measurement***. We then use a sparse recovery algorithm under the CS framework to estimate the target tag's position. Specifically, the algorithm tries to find a one-dimensional vector, whose multiplication production with the fingerprint matrix is as close as possible to the real-time measurement vector. The found vector is essentially the sparse location vector that we are looking for. An element with a value of '1' in the location vector then indicates the estimated position or location id for the target tag.

However, performing the recovery algorithm on a large fingerprint matrix could be expensive. To reduce the computational overhead, we decouple the problem into two sub-problems. We first divide the deployment region into subareas (e.g., different book shelves in a library), so that each subarea contains a subset of the object tags – on which a smaller fingerprint matrix can be constructed. To locate a tag, we first use an offline learned classifier to predict which subarea the target tag belongs to, and then apply the sparse recovery algorithm to the smaller fingerprint sub-matrix to quickly find the location vector. This divided-and-conquer strategy allows our algorithm to scale to a large RFID deployment.

A natural question is: "*how many reference tags are needed*"? Deploying too many reference tags will waste money and time, but having too few of them will result in poor performance. In this paper, we prove that organizing the reference tags as a mesh of equilateral triangles is the most cost-effective way to achieve high precision; we then design a heuristic to determine the minimum number of reference tags and how to organize them in a specific region.

We have developed a prototype of CSRP and evaluated it in a library room with rich multipath and NLOS effects. Experimental results show that CSRP is able to correctly locate 84.7% of the test items with an average location accuracy of less than ten centimetres across all test items. This performance is comparable to PinIt, but CSRP uses an order of magnitude less reference tags and does not rely on specialize hardware.

This paper makes the following contributions:

- We present a novel RFID-based positioning system. Our system offers high positioning precision but requires an order of magnitude less reference tags than the state-of-the-art. As a result, it saves cost and time in a large-scale deployment.
- Our work is the first to employ compressive sensing for RFID-based positioning.
- We show how to translate our novel idea to a practical system. We present new analysis and algorithms to calculate the optimal number of reference tags as well as the best way for organizing reference tags.
- Our approach is immediately deployable on off-the-shelf RFID hardware.

## II. OUR APPROACH

### A. Overview

Fig. 1 illustrates a high-level overview of CSRP, which consists of four offline and online stages described as follows.

**Offline Deployment and Data Collection**: The first step is to deploy a number of reference tags in the deployment site. We then collect the signal phase readings for all object tags and reference tags. This process only needs to perform once. If an object tag is replaced, we recollect the phase reading of the new tag. If a tag is removed, we delete it from our database. We show that placing the reference tags at the intersections of a mesh of equilateral triangles gives the best cost-effective performance. See Section II-D.

**Offline Fingerprint Matrix Construction**: After collecting the data for each tag, we fingerprint each object tag by calculating the spatial relation between the object tag's multipath profile and each reference tag's. This process gives us a fingerprint matrix for all object tags. See Section II-C.

**Online Measurement Vector Acquisition**: To locate an item with an known tag ID, we first use an RFID reader to track the RF signal associated with the tag ID. We take the real-time signal phase measurement of the target and each reference tag. The measurements are then used to compute the real-time spatial relation between the target and reference tags. This results in a real-time measurement vector.

**Online Target Tag Positioning**: The real-time measurement is fed into a machine learning classifier to predict which subarea the target tag belongs to. We then use a sparse recovery algorithm to take in the real-time measurement and the fingerprint matrix of the predict subarea to estimate the location of the target object. See Section II-E.

### B. Problem Formulation

Fig. 2 depicts an example deployment setup of our approach. In this example, there are in total $N$ objects where each object is attached with an RFID tag. We also deploy $M$ $(M < N)$ reference tags. Suppose that there are $K$ target

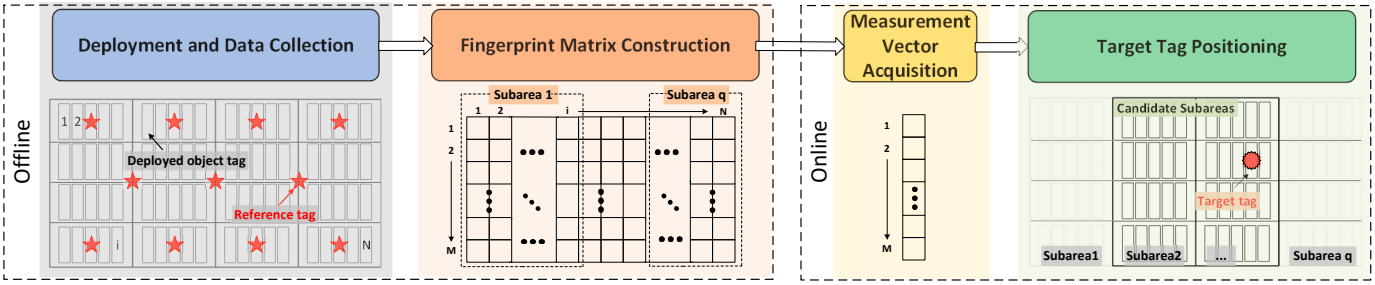


Fig. 1: Overview of CSRP. At the offline deployment phase, the object tags and a few number of reference tags are deployed in the entire region, and CSRP automatically calculates the fingerprint matrix. During online localization, CSRP obtains a measurement vector, predicting which subarea the target tag belongs to, and then using the measurement together with the fingerprint matrix to derive a location vector that indicates the target's location.

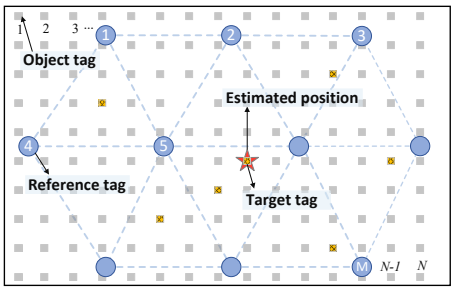


Fig. 2: An example CSRP deployment setup with $N$ object tags and $M$ reference tags. Unlike [6], the number of reference tags is signifantly less than the total number of object tags, i.e., $M < N$.

tags that we want to locate. These target tags are randomly distributed among $N$ objects. We use a location vector $\Phi$ to represent the positions of $K$ tags as:

$$\boldsymbol{\phi} = [\phi(1), \cdots, \phi(j), \cdots \phi(N)]^T, \tag{1}$$

where $\phi(j) \in \{0, 1\}$, and when the tag is in position $j$ when $\phi(j) = 1$, and is not in position $j$ when $\phi(j) = 0$. We want to highlight that the number of target tags is equal to the number of non-zero elements in vector $\Phi$, i.e., $K = \sum_{j=1}^{N} \phi(j)$. If the number of target tags, $K$, for which we want to locate at a given moment is significantly smaller than the total number of object tags, $N$, then the location vector, $\Phi$, will be a sparse vector. Based on the sparse property of $\Phi$ and according to the CS theory in sparse recovery [13], when the number of target tags is 1 (i.e., locating one object at a time), the tag positioning problem can be formulated as:

$$\mathbf{y}_{M\times 1} = \mathrm{X}_{M\times N} \cdot \boldsymbol{\phi}_{N\times 1} + \mathcal{N}, \tag{2}$$

where $\mathbf{y}_{M\times 1}$ is the real-time measurement vector, and $\mathrm{X}_{M\times N}$ is the fingerprint matrix, and $\mathcal{N}$ is the measurement noise. According to prior studies [11]–[14], when the fingerprint matrix satisfies the restricted isometry property (RIP), the location vector can be accurately recovered by solving Equation (2).

While the above formulation assume locating one object at a time, our approach can also be extended to solve a multiple-target positioning problem (i.e., when $K$ is greater than 1). Because the readings of different tags can be separated using their IDs (which are given to the RFID reader), we can simplely estimate the position of each tag one by one. Specifically, each tag would have its own real-time measurement vector, $\mathbf{y}$, and a generated location vector, $\boldsymbol{\phi}$. Thus, Equation (2) can be re-defined as:

$$\begin{aligned} &Y_{M\times K} = \mathrm{X}_{M\times N} \cdot \Phi_{N\times K} + \mathcal{N}, \\ &\mathrm{X} = [\mathbf{x}_1, \cdots, \mathbf{x}_j, \cdots, \mathbf{x}_N], \mathbf{x}_j \in \mathbb{R}^{M\times 1}, \\ &Y = [\mathbf{y}_1, \cdots, \mathbf{y}_j, \cdots \mathbf{y}_K], \mathbf{y}_j \in \mathbb{R}^{N\times 1}, \\ &\Phi = [\boldsymbol{\phi}_1, \cdots, \boldsymbol{\phi}_j, \cdots \boldsymbol{\phi}_K], \boldsymbol{\phi}_j \in \mathbb{R}^{N\times 1}. \end{aligned} \tag{3}$$

where $\mathbf{x}_j$ is the fingerprint of target tag $j$, and $\mathbf{y}_j$ and $\boldsymbol{\phi}_j$ are the measurement and the location vector, respectively.

As shown in Equation (3), only measurements of $M$ reference tags are used for positioning. By contrast, PinIt would have to collect the phase readings from at least $N$ reference tags (where $N$ is equivalent to the total number of object tags) [6]. Therefore, CSRP reduces the number of measurements by $\frac{N-M}{N}$ $(M < N)$ when compared with PinIt. The reduction can save the deployment cost and alleviate signal conflicts in a large-scale deployment.

### C. Fingerprint matrix construction

Following the common practice in RFID positioning [1], [5], [6], CSRP also use the signal fingerprint of tags to locate a specific object. There are two types of signal measurments can be directly obtained from an object tags using a RFID reader, RSS and the phase. We choose to use the phase to construct the fingerprint because it is more robust to the multipath effect and NLOS when compared to RSS [6].

In this paper, we use the multipath profile [6] as a measurement feature for each tag. Formally, a multipath profile is a vector, $P(\theta)$, which records the power of the tag's received signal in the beam with a given direction, $\theta$ (where $\theta \in [0°, 180°]$). Given a reader with $Q$ uniformly spaced antennas as shown in Fig. 3(a), the received signal will be projected by each antenna to obtain a narrow beam in the $\theta$ direction. Therefore, the multipath profile, $P(\theta)$, collected

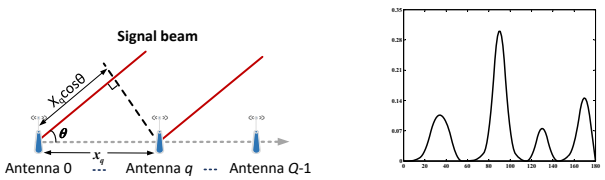


(a) Beam steering.

(b) A multipath profile.

Fig. 3: Collecting the phase readings for feature extraction.

from the $\theta$ direction can be obtained using the following formula [6]:

$$P(\theta) = \left|\sum_{q=0}^{Q-1} w(q,\theta) \cdot s_q\right|^2, \tag{4}$$

$$w(q,\theta) = e^{-j\frac{2\pi}{\lambda} \cdot x_q \cos\theta}, \tag{5}$$

where $s_q$ is the tag's signal observed from the $q^{th}$ antenna, $w(q,\theta)$ is the weight to $s_q$ when steering the beam to direction $\theta$, and $\lambda$ is the wave length and $x_q$ is the position of the $k^{th}$ antenna.

Traditional fingerprint methods suffer from low accuracies due to subtle environmental changes. In this work, we take a different fingerprint approach to avoid the problem. Specifically, we compute the spatial relation of each object tag with respect to the reference tags. Because the spatial relationship keeps unchanged as long as the relative position between tags remains stable, we can use the spatial similarities between the object and the reference tags as the fingerprint to cancel the environmental noise. To compute the spatial similarity, we use the dynamic time warping (DTW) distance [15], a widely used similarity metric for time series. Formally, the fingerprint for the object tag $j$ can be represented as a column vector:

$$\mathbf{x}_j = [x_{1j}, \cdots, x_{ij}, \cdots, x_{Mj}]^T,$$
$$x_{ij} = \|P_j(\theta) - P_{r_i}(\theta)\|_{DTW}, \tag{6}$$

where $P_j(\theta)$ and $P_{r_i}(\theta)$ are the multipath profiles of the $j$-th object tag and the $i^{th}$ reference tag, $\|\cdot\|_{DTW}$ quantifies the similarity of multipath profiles between them [6].

**Fingerprint Matrix.** After collecting the multipath profiles of $N$ object tags, a fingerprint matrix, X, of $M$ rows and $N$ columns can be constructed. Here, $M$ and $N$ are the number of reference and object tags respectively, and each column of $X$ is represented as $\mathbf{x}_j$ in Equation (6).

**Online Measurement Vector Acquisition.** To locate a specific tag, we collect the phase readings of the target tag and the reference tags within a region by exploiting Equation (6). Here, the real-time measurement vector, $\mathbf{y}_j$, for a target tag, $j$, is defined as:

$$\mathbf{y}_j = [y_j(1), \cdots, y_j(i), \cdots, y_j(M)]^T,$$
$$y_j(i) = \|P_j(\theta) - P_{r_i}(\theta)\|_{DTW}, \tag{7}$$

where $y_j(i)$ is the DTW distance between multipath profiles of the target tag and reference tag $i$.

The rationales for representing the fingerprint matrix X in the form described in Equation (6) are explained as follows. Firstly, the fingerprint matrix can have either $N$ or $M$ rows, where $N$ and $M$ are the number of object and reference tags respectively. We choose to use a $M$-row representation because this allows us to recover the location vector, $\boldsymbol{\phi}_j$, of object tag $j$ using a smaller number of real-time measurements – recall that $M < N$. To this end, we calculate the multipath profile distances between each location and $M$ reference tags and use them as the fingerprint, i.e., row $j$ of the fingerprint matrix becomes the fingerprint of object tag $j$. Secondly, the measurement vector $\mathbf{y}_j$ is the inner product of the location vector $\boldsymbol{\phi}_j$ and row $i$ of the fingerprint matrix, thus $\mathbf{x}_i$ should include all the multipath profile distances between reference tag $i$ and the $N$ object tags. Finally, the fingerprint matrix will obey the restricted isometry property (RIP), which is the sufficient condition to conduct CS recovery. Proof and steps for computing the location vector, $\theta$, are given in Section II-E.

### D. Offline Reference Tag Deployment

In this subsection, we will introduce the principals for deploying reference tags. We present two theorems that provide guidance on how to deploy reference tags to achieve a good performance in a cost-effective manners. In particular, we want to answer two specific questions: "*how many reference tags are needed?*" and "*how should they be deployed?*".

*1) How many reference tags are needed?:* In a practice, the number of target tags, $K$, to be positioned is known. According to the CS theory, we need as few as $K\log(N/K)$ measurements to accurately recover a $K$-sparse location vector, $\boldsymbol{\phi}$, for $N$ object tags. Because $K\log(N/K) \leq M < N$ (when all the terms are no less than 1), the number of reference tags needed, $M$, is smaller than the number of object tags, $N$. Compared with PinIt which requires at least $N$ reference tags to, CSRP significantly reduces the deployment cost by relying on less reference tags. Furthermore, using less reference tags also has the benefit of reducing the data collisions among tags, as shown in Section IV-D.

*2) How to deploy reference tags?:* There are two challenges of reference tag deployment. The first one is to avoid placing redundant reference tags that carry similar information. To do so, we need to make sure the distance between any two reference tags are as large as possible. As a result, the neighboring rows in the fingerprint matrix will have the maximum distinct value. The second challenge is to make sure the resultant fingerprint matrix can effectively capture the subtle difference between two nearby object tags which have similar multipath readings. To do so, we need to maximize the difference between neighboring columns in the fingerprint matrix. The neighboring columns are fingerprints of two nearby object tags, doing so allows us to match the real-time measurement vector to the fingerprint column of correct object tag. To this end, we would like the distance between one object tag and its nearest reference tag to as small as possible. By mapping each object tag a distinct, nearest reference tag (i.e., the one with the smallest multipath distance to the object tag), the smallest element of any two columns will have a different vector index (as the nearest reference tag for two object tags are different).

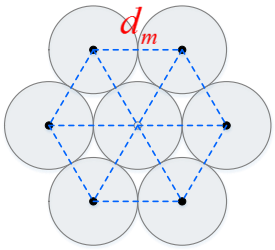


Fig. 4: Deployment of theorem 1.

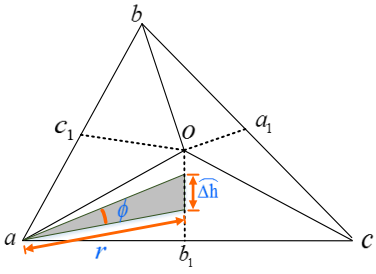


Fig. 5: Deployment of theorem 2.

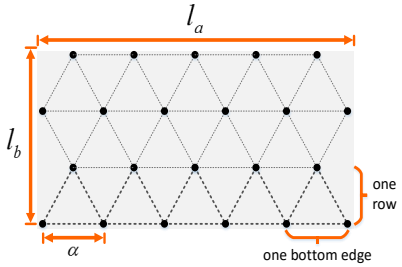


Fig. 6: Deployment of triangles.

After that, the neighboring columns reveal a discriminative feature.

After describing our strategy for reference tag deployment, we now provide two theorems to prove that an effective deployment can be achieved when the reference tags form a mesh of equilateral triangles. The proofs are similar to the one presented in [16] for choosing measurement points.

*Theorem 1:* The distances between each pair of reference tags can be maximized when they are at the intersections of a mesh of equilateral triangles.

*Proof 1:* Given the number of reference tags and the deployment area, the theorem can be proven through its opposite proposition. We just need to prove that when the distance of neighboring reference tags is fixed, the deployment area can be minimized if the reference tags are deployed at the intersections of a mesh of equilateral triangles. Note that when the reference tags are evenly deployed, the area can be divided into acute or right neighboring triangles[1].

Suppose that the distance between neighboring reference tags is $d_m$, and we draw circles centering on each reference tags with radius $d_m/2$ and there is no overlap between them, as shown in Fig. 4. According to the Thue's Theorem, the ratio between the total area of these triangles $S_m$ and the area of the deployment region $S$ is restricted to $\pi/\sqrt{12}$ as:

$$S_m/S = 2M\pi(0.5d_m)^2/S \leq \pi/\sqrt{12}, \tag{8}$$

$$S \geq \sqrt{3}Md_m^2, \tag{9}$$

and when the edge length $d_m$ of the triangles are equivalent, $S$ achieves its minimum value with $\sqrt{3}Md_m^2$. This proves that the deployment of reference tags with equilateral triangles maximizes the distance between reference tags.

*Theorem 2:* When the deployment of reference tags are a mesh of equilateral triangles, the distance between each tag and its nearest reference tag can be minimized.

*Proof 2:* Since the area can be divided into triangles, each tag can be treated as uniformly distributed in one of the triangles. Suppose the tag $p$ is located in $\Delta abc$, as shown in Fig. 5, $oa_1$, $ob_1$ and $oc_1$ are three midperpendiculars of edge $bc$, $ac$ and $ab$, respectively. Thus the nearest reference tag to $p$ is $a$, $b$ or $c$ if $p \in \square ab_1oc_1$, $\square ba_1oc_1$ or $\square ca_1ob_1$, respectively.

To proof the theorem, we compute the expected distance between $p$ and it's nearest reference tag first. Let $E_{pa}$ denote the expected distance between $p$ and $a$ in $\Delta aob_1$, $S_{\widehat{\Delta h}}$ and $S_{a\widehat{\Delta h}}$ denote the area of radian $\widehat{\Delta h}$ and sector $a\widehat{\Delta h}$ respectively:

$$\begin{aligned} E_{pa} &= \frac{1}{|ob_1|}\int_0^{|ob_1|} \frac{S_{a\widehat{\Delta h}}}{S_{\widehat{\Delta h}}} d\widehat{\Delta h} \\ &= \frac{1}{|ob_1|}\int_0^{|ob_1|} \frac{\int_0^{\phi}\int_0^{r} x^2 d\Delta r d\Delta\phi}{r^2\phi/2} d\widehat{\Delta h} \\ &= \frac{|oa|}{3} + \frac{|oa|\sin^2\angle aob_1}{3\cos\angle aob_1}\ln\left(\cot\frac{\angle aob_1}{2}\right). \end{aligned} \tag{10}$$

In the same way, the expected distance between $p$ and $b$ in $\Delta boc_1$, $p$ and $c$ in $\Delta coa_1$ can be obtained. Since $S_{\Delta aob_1} = S_{\Delta aoc_1}$, $S_{\Delta boc_1} = S_{\Delta boa_1}$, $S_{\Delta coa_1} = S_{\Delta cob_1}$ and $|oa| = |ob| = |oc|$, the expected distance between $p$ and its nearest reference tag in $\Delta abc$ can be obtained by:

$$E_p = \frac{2(E_{pa}\cdot S_{\Delta aob_1} + E_{pb}\cdot S_{\Delta boc_1} + E_{pc}\cdot S_{\Delta coa_1})}{S_{\Delta abc}}, \tag{11}$$

as $S_{\Delta aob_1} = |oa|^2\sin 2\angle aob_1/4$, $S_{\Delta boc_1} = |oc|^2\sin 2\angle boc_1/4$, $S_{\Delta coa_1} = |oc|^2\sin 2\angle coa_1/4$ , (11) becomes:

$$\begin{aligned} E_p = &\frac{1}{3}\sqrt{\frac{2S_{\Delta abc}}{\sin 2\angle aob_1 + \sin 2\angle boc_1 + \sin 2\angle coa_1}} \\ &+ \frac{2}{3}\sqrt{\frac{2S_{\Delta abc}}{(\sin 2\angle aob_1 + \sin 2\angle boc_1 + \sin 2\angle coa_1)^3}}\cdot \\ &\Big(\sin^3\angle aob_1\ln(\cot\frac{\angle aob_1}{2}) + \sin^3\angle boc_1\ln(\cot\frac{\angle boc_1}{2}) \\ &+ \sin^3\angle coa_1\ln(\cot\frac{\angle coa_1}{2})\Big). \end{aligned} \tag{12}$$

As $S_{\Delta abc}$ is fixed, $E_p$ can be minimized if and only if $\angle aob_1 = \angle boc_1 = \angle coa_1 = \pi/3$. Finally, the expected distance is minimized.

Now we discuss how to choose the edge length of the triangles to accurately recover the location vector. As shown in Fig. 6, suppose a rectangular region with a size of $l_a \times l_b$ (where $l_a$ and $l_b$ are the length and width respectively). Suppose the region is divided into $\gamma$ rows of equilateral triangles, and the maximum number of the bottom edge for one row is $\beta$. Let $\alpha$ represents the edge length of one triangle. The segmentation goal is to make the triangles cover as much areas of the region as possible, while at the same time to meet the following three conditions: (a) the number of triangles vertexes is equal to the number of reference tags and $M \geq O(K\log(N/K))$; (b) the total length of bottom edges for $\beta$ triangles should smaller than

[1]The evenly deployed reference tags are bound to form a mesh of parallelograms, and any parallelogram can be divided into two acute or right triangles.

the region length; and (c) the total length of triangle heights for $\gamma$ rows should be smaller than the region width.

The edge length $\alpha$ for each triangle can be obtained by solving the following linear programming problem:

$$\begin{array}{l} \max \ \ \beta \times 2\gamma \times \frac{\sqrt{3}}{4}\alpha^2, \\ \left\{ \begin{array}{l} (\beta+1) \times (\gamma+1) \leq M, \\ \beta \times \alpha \leq l_a, \\ \gamma \times \frac{\sqrt{3}}{2}\alpha \leq w_b. \end{array} \right. \end{array} \tag{13}$$

### *E. Target Tag Positioning*

We first present the detailed positioning process. Then we prove that the fingerprint matrix satisfies the RIP with a high probability.

*1) Locating the target tags:* One of our goals is to design a highly accurate recovery algorithm that has a low time complexity, so that it can be applied to large-scale deployments. If we directly apply the sparse recovery algorithm on the fingerprint matrix, it will cause high computation cost. This problem will be exacerbated when the number of deployed object tags increases. Besides, we prefer to provide a more user-friendly result like "the object is at shelf $i$, rack $j$, and position $k$" rather than a general answer like "the object is at position $k$". Considering these reasons, we propose a hierarchical algorithm which consists of two steps.

In the first step, we divide the fingerprint matrix into sub-matrices corresponding to different subareas (e.g., shelves). We apply the marginal fisher analysis (MFA) [17] to the fingerprint matrix to train a classifier. The target tag is first positioned to two candidate subareas in this step. We have also explored several alternative classification techniques. This is discussed in Section IV-G. In the second step, we apply the sparse recovery algorithm on the candidate sub-matrices to recover the location vectors for multiple target tags. Each target tag's real-time measurement vector is used to recover the location vector. To get a high accuracy, we utilize the popular orthogonal matching pursuit (OMP) algorithm which is robust to errors and noise [18].

We now describe the two steps in more details.

*2) Step 1: Predicting the target tag's subarea:* MFA is a widely used supervised classification algorithm. It works by projecting samples into a subspace, so that the samples in the same class are made as compacted as possible, and the different classes are made as far as possible. To model the intra-class compactness, MFA constructs an intrinsic graph where each sample is connected to its $k_1$ nearest neighbors in the same class. Then, a penalty graph is constructed to describe the adjacency relationship between inter-class marginal samples [19]. By minimizing the ratio of the intrinsic graph and penalty graph, each target tag can be pointed into a specific subarea.

Specifically, we term each fingerprint (a column vector) as a sample $\mathbf{x}$, and $E_{ij}^{IN}$ represents the weight of sample $\mathbf{x}_i$ and $\mathbf{x}_j$, which in the same class. $E_{ij}^{IN} = 1$, if $\mathbf{x}_j$ is a $k_1$-nearest neighbor of $\mathbf{x}_i$ or vice versa; otherwise, $E_{ij}^{IN} = 0$. Similarly, the weight between different class samples $\mathbf{x}_i$ and $\mathbf{x}_j$ is $E_{ij}^{P} = 1$, if $\mathbf{x}_j$ is a $k_2$-nearest neighbor of $\mathbf{x}_i$ or vice versa; and $E_{ij}^{P} = 0$ otherwise. Moreover, if the number of subareas is $L$, the MFA subspace minimizes:

$$\begin{aligned} \mathrm{Y}(W) &= \frac{\sum_{i=1}^{L}\sum_{j=1}^{L}(W^T\mathbf{x}_i - W^T\mathbf{x}_j)^T(W^T\mathbf{x}_i - W^T\mathbf{x}_j)E_{ij}^{IN}}{\sum_{i=1}^{L}\sum_{j=1}^{L}(W^T\mathbf{x}_i - W^T\mathbf{x}_j)^T(W^T\mathbf{x}_i - W^T\mathbf{x}_j)E_{ij}^{P}} \\ &= \frac{tr\left(W^TX\left(D^{IN} - E^{IN}\right)W^TX\right)}{tr\left(W^TX\left(D^{P} - E^{P}\right)W^TX\right)} \end{aligned} \tag{14}$$

where $D^{IN}$ and $D^{P}$ are diagonal matrices with the $i$th entry $D_{ii}^{\mathrm{IN}} = \sum_{j=1}^{N} E_{ij}^{IN}$ and $D_{ii}^{\mathrm{P}} = \sum_{j=1}^{N} E_{ij}^{P}$.

$$W = \arg\min_{W} Y\left(W\right), \tag{15}$$

and $Y(W)$ is the direction of the linear projection. To ensure the following positioning accuracy, each time we choose two candidate subareas to be processed in the experiment.

*3) Step 2: Positioning using the sparse recovery algorithm:* In this step, the measurement vector of each target tag together with the candidate sub-matrices are used to recover the location vector. Due to data lost and noise during signal propagating, the measurement vector for one tag will mismatch the fingerprint. This problem be will exacerbated in a large-scale deployment. To tackle this problem, we leverage OMP, a simple but robust recovery algorithm, to accurately position the target tags:

$$\begin{aligned} &\min \|\hat{\Phi}\|_2, \\ &s.t. \ \|\mathrm{X}^{\dagger}(\mathrm{Y} - \mathrm{X}\hat{\Phi})\|_2 < \delta. \end{aligned} \tag{16}$$

It has been proven that the location vector, $\boldsymbol{\phi}_k$, can be accurately recovered by the OMP algorithm if the fingerprint matrix X satisfies (1) the RIP and (2) the dimension of measurement vector $\mathbf{y}_k$ for the $k$-th target tag, and (3) obeys $M = O(K\log(N))$ (where $M$ and $N$ are the number of reference and object tags respectively) [18].

**Complexity Analysis.** We now discuss the computation complexity of our recovery algorithm. The complexities of MFA and OMP are $O(L^2)$ and $O(KMN)$, respectively. Our hierarchical algorithm combines both algorithms and has a complexity of $O(L^2 + \frac{KMN}{L})$. Note that the number of subareas is usually smaller than the number of reference tags, that is $L < M$ and $M < N$. As a result, the complexity of our algorithm is approximately $O(\frac{KMN}{L})$. When compared with the case of solely applying OMP algorithm which has a complexity of $O(KMN)$, our algorithm reduces the complexity a factor of $L$.

*4) Meeting the RIP constraint:* Finally, we show that the fingerprint matrix X is highly likely to satisfy the RIP constraint.

*Theorem 3:* When the number of reference tags satisfies $M = O(K\log N)$ and each row $\mathbf{x}_i$ ($i \in [1, M]$) in the fingerprint matrix is independently and identically distributed, X satisfies the RIP defined as [11], [13]:

$$(1-\delta) \leq \|\mathrm{X}\Phi\|_2^2 / \|\Phi\|_2^2 \leq (1+\delta). \tag{17}$$

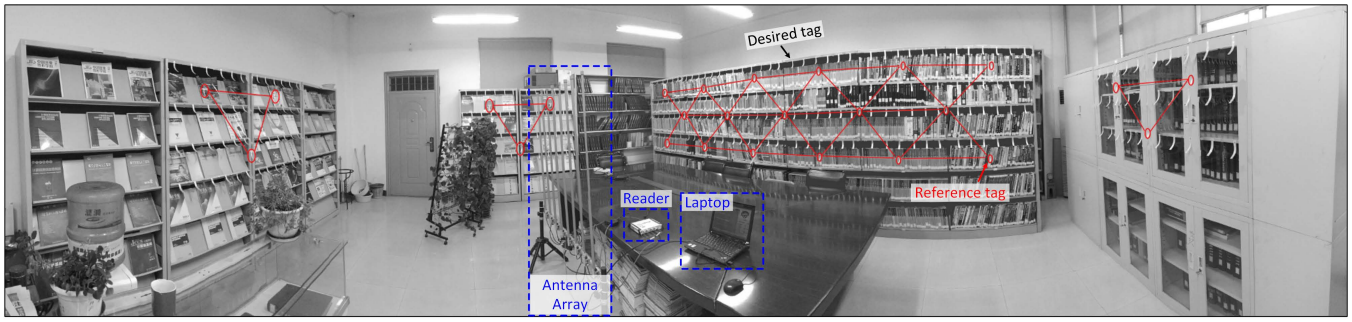


Fig. 7: Experiment deployment layout. The antenna array is deployed at the middle region of the library room. We choose 12 racks to deploy object tags and the reference tags. There are in total 270 object tags and 26 reference tags deployed.

for a $N$-dimensional $K$-sparse matrix $\Phi$ which tends to 1, where $\delta \in (0, 1)$.

## III. Experimental Setup

### A. Hardware

Our system is built upon omnidirectional antennas and commercial UHF RFIDs. We use a commercial off-the-shelf contactless RFID reader to track tags.

**RFID Reader.** We use an ImpinJ Speedway RFID reader (modeled R420) [20] during test. This reader is compatible with the EPC Gen2 standard [21], operating in the frequency range of 920.5–924.5 MHz. We did not modify any hardware component or firmware of the reader.

**Antenna Array.** We deployed eight Q900F-900 omnidirectional antennas [22] to form a linear antenna array with a 16 cm half-wavelength space between adjacent antennas. Each antenna offers a communicate range of around 12 meters even when the RFID devices backscatter a week signal.

**Tags**: We use the Alien Squiggle General Purpose UHF RFIDs as object and reference tags. These are passive backscatter RFIDs working in the UHF band, but other passive RFIDs can also be used. Furthermore, reference tags are placed at the selected reference positions (found using the heuristic described in Section II-D), which are expected to remain unchange throughout their lifetime.

### B. Evaluation Scenarios

**Evaluation Environment.** We evaluate our approach in an indoor library room with rich multipath and NLOS. The working area of the experimental area is of size 5 m $\times$ 8 m. The reference tags and object tags are deployed on 12 racks (46 book shelves), as shown in Fig. 7. The racks are made of mental and wood. The reference tags are set at the vertex of the equivalent triangles to cover the whole test region. Note that we did not put any tags outside of the shelves, so there are no tags except for the reference and object tags. Each wall of the indoor room is attached with shelves and each shelf is full of books, resulting in a complex multipath environment. We stress that there is not specific requirement on how the RFID reader should be placed, as long as it can read tags.

**Offline Data Collection.** Recall that our approach uses a fingerprint matrix to locate objects (Section 1). To construct the fingerprint matrix, we first use the RFID reader to read data of each tag to obtain its multipath profile. Next, we calculate the DTW values between the multipath profiles of each object tag and reference tags. Because tags in a rack have similar spatial features which are different from those located in a different rack, we group tags of one rack to a subarea. Applying this strategy breaks our experimental environment into 12 subareas.

**Competitive Approach.** We compare our approach against PinIt, a state-of-the-art RFID-based positioning system [6]. We faithfully repeated PinIt's setup in our deployment site, by evenly distributing reference tags between objects. In total, we have placed 285 reference tags for PinIt. To locate an object tag, PinIt selects a reference tag (whose location is known ahead of time) which has a multipath profile that is most similar to the target tag's, and then uses the selected reference tag to estimate the target tag's location.

**Evaluation Methods.** We have conducted extensive experiments to evaluate the performance of CSRP, and compare it with PinIt. We also evaluate the deployment cost and data collisions of both approaches, and analyze the working mechanism of our approach. To provide a fair comparison, we have used all deployed objects as test items in our experiments.

## IV. Experimental Results

In this section, we first present the overall accuracy of CSRP, showing that it achieves a similar accuracy as the state-of-the-art. Next, we evaluate the effectiveness of our sparse recovery algorithm, and how does the number of reference tags affects positioning accuracy, data collisions, and deployment cost. We then show that CSRP works effectively in LOS and NLOS environments, before discussing the alternative modeling techniques for subarea predictions.

### A. Overall Performance

From Fig. 8, both CSRP and PinIt achieve a good positioning accuracy. Both approaches are able to correctly identify the location id for 84.7% and 86.4% of the test items respectively. For 95% of the object tags, the average location accuracy of

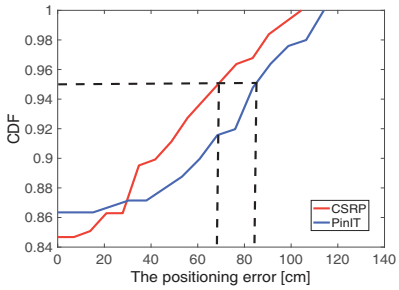


Fig. 8: Overall positioning accuracy.

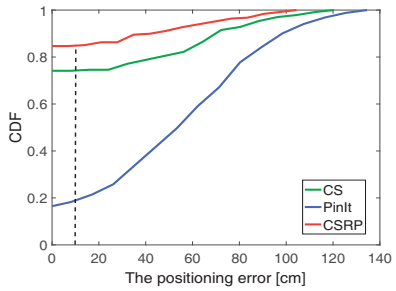


Fig. 9: Different positioning methods.

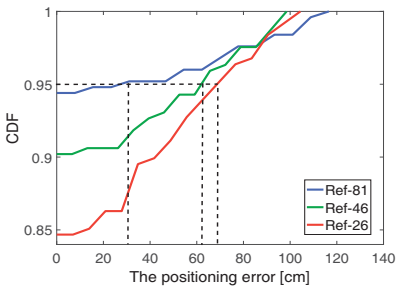


Fig. 10: Impact of number of RTs.

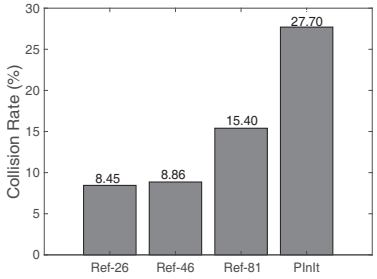


Fig. 11: Tag collision comparison.

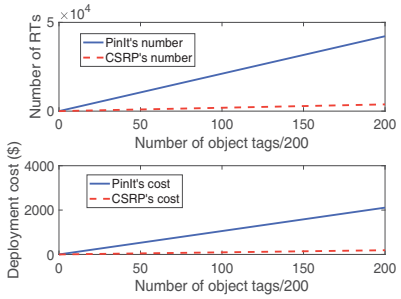


Fig. 12: Deployment cost comparison.

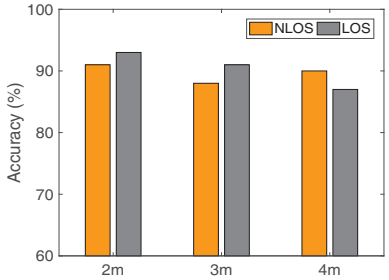


Fig. 13: Impact of different environments.

CSRP is within 7cm. This is slightly better than the average accuracy of 8.5cm given by PinIt. This improvement is largely due to the fact the CSRP uses significantly less reference tags (26 vs 285) and the spatial relation to cancel the environmental noise, which in combination reduces the negative impact of data collisions. Overall, CSRP delivers a similar positioning performance when compared with PinIt, but uses an order of magnitude less reference tags.

### B. Comparison of Positioning Recovery Methods

In this experiment, we compare our sparse recovery algorithm against two alternatives: a standard CS approach and the DTW-based matching method used by PinIt. In this evaluation, we use the 26 reference tags deployed under our scheme for positioning.

The Cumulative Distribution Function (CDF) chart in Fig. 9 describes how positioning accuracy for each method changes as the accepted location error changes. If we consider a location error of less than 10 cm as acceptable, then CSRP gives an accuracy of 87.9%. Under this assessment criterion, the traditional CS method and PinIt give an accuracy of 74.9% and 17% respectively. Clearly, CSRP outperforms both approaches. If we relax the assessment criteria to allow the positioning error to be less than 80cm, the sparse recovery algorithm still remains the best method among the three approaches.

We can also see from the diagram that CS-based methods significantly outperforms PinIt. This is largely because PinIt needs a large number of reference tags to work efficiently. For the CS method, owning to its high robustness against the environment noise, it delivers reasonably good performance. Our approach enhances the standard CS scheme by first predicting which of the subareas the target tag belongs to. This prediction helps us in removing most of the outliers from the candidate locations, leading to better performance. Note that there is a huge accuracy decline for PinIt when considering the accuracy of 13 cm reported in [6] when using many more reference tags.

### C. Impact of The Number of Reference Tags

In this experiment, we deploy 26, 46 and 81 reference tags in the our evaluation scene and test how does the number of reference tags (RTs) affect the positioning accuracy of CSRP. Fig. 10 shows the corresponding positioning errors under different reference tag configurations. When using 26 reference tags, 84.7% of the target tags are positioned in the correct positions. While for the cases of 46 and 81 reference tags, the number of correctly positioned target tags are 90.2% and 94.3%, respectively. For 95% of the testing tags, the positioning error for configurations using 26, 46 and 81 reference tags are within a distance of 7 cm, 6.3 cm and 3.2 cm, respectively. Using more reference tags indeed improves the positioning accuracy, but our approach uses many fewer reference tags when compared with PinIt.

### D. Data Collisions

In order to quantify the data collision between tags (both the reference tags and the object tags) under four different deployment cases, we calculate the collected data rate $\omega$ within a time period to measure the collision probability. Specifically, $\omega$ is computed as $\omega = \frac{S_{all}-S_{rec}}{S_{all}}$, where $S_{all}$ is the sum of the number of deployment tags and $S_{rec}$ is the total number of tags received by the reader. Here, $S_{all}$ and $S_{rec}$ both contain

TABLE I: Classification accuracy per model

| Classifier | Accuracy (%) | Classifier | Accuracy (%) |
|---|---|---|---|
| Naive Bayes | 85.2 | SVM | 91.2 |
| MLP | 88.1 | KNN | 85.4 |
| Decision Tree | 89.2 | ANN | 89.6 |
| MFA | 100 | | |

the data of object tags and reference tags. Fig.11 shows that the collision probability increases with more tags, i.e., using a smaller number of reference tags leads to fewer tag collision when the number of object tags remains the same. By using fewer reference tags, CSRP can thus reduce the tag collision by deploying fewer and sparsely distributed reference tags.

### *E. Deployment Cost*

To compare the deployment cost, we calculate how many reference tags is needed by CSRP and PinIt as the number of object tags changes. Fig.12 shows how does the deployment cost increase as the number of reference tags increases, where we assume each tag costs $ 0.05. With the default setup, CSRP needs 19 reference tags when the number of object tags is 200. While PinIt needs in total 496 reference tags for the same scenario. When the total number of object tags reaches 40,000, the number of reference tags (RTs) and deployment cost for CSRP and PinIt are 3,800, $190 and 4,2200, $2,110, respectively. As a result, CSRP saves 91.0% of the deployment cost when compared with PinIt. This massive reduction also means that there will be less human involvement in installing and maintaining the reference tags.

### *F. Performance of LOS and NLOS environments*

To evaluate the effectiveness of our system in different environments, we place 11 reference tags and 150 object tags on four movable shelves. To mimic a LOS setting, we put the book shelves in an empty hall. For NLOS environment, we block the direct paths by setting the shelves in an office environment. The results are shown in Fig.13. We can observe from the diagram that: i) CSRP achieves a positioning accuracy of around 90% in both LOS and NLOS when the tags are spaced within a range of 2 m to 8 m. ii) it achieves consistently accurate performance regardless the distance between the tag and the RFID reader.

### *G. Alternative Classification Methods for Subarea Prediction*

Table I gives the sub-area prediction accuracy of various alternative classification techniques and our RF model. The alternative models were built using the same features and training data. Due to the high-quality features, all classifiers deliver reasonably good prediction accuracy. We choose MFA because it gives the best prediction accuracy and is proven to be effective in modeling time series data [17].

## V. RELATED WORK

Localization is a key enabling technique underpinning many applications including sensor networks [23], [24], smart homes [25] and IoTs (Internet of things) [26]. This section reviews some of the most relevant works for the RFID positioning.

**RSS Based Methods.** RSS reflects the received signal strength in the power level. Early systems [1], [4] locate a tag with the help of some anchor tags whose locations are known. To estimate the location of a target tag, these approaches compare the RSS measurement of a target tag with a set of deployed reference tags. To the anchor-free localization, the work presented by Yang *et al.* [27] tries to model the signal propagation in a complex environment. Other work [3] combines the RSS and the tag's reading rate to design a tag order identification system. However, RSS is sensitive to the multipath or NLOS path environment [28] and its accuracy highly depend on the antenna gain and tag orientation. As a result, these systems often have a poor localization accuracy in practice [5].

**Phase Based Methods.** The signal phase indicates the distance that a wireless signal goes through. Phase based methods can be generally divided into two categories, AOA (Angle of Arrival) and SAR (synthetic aperture). AOA based systems [8]–[10] locate the target tag by measuring the phase differences of different antennas. The major drawback for an AOA approach is that it gives poor performance in a multipath environment. Wang *et al.* [29] track the trajectory of the target tag using grating lobes to overcome the limitation of AOA. However, their approach cannot decide the absolute position of the object tag. To reduce the hardware cost, other researchers [30]–[33] utilize SAR to simulate multiple antennas. For example, Minsen *et al.* [32] employs a moving antenna to simulate the SAR to locate the target by constructing a hologram. Similarly, PinIt [6] exploits the moving antenna and locates the target tag by comparing the multipath profile using a large number of reference tags. Benefiting from the SAR method, PinIt is able to locate the target tag with a sub-meter level accuracy in the NLOS path and a rich multipath environment. However, the large number of reference tags required by PinIt not only incurs high deployment cost, but also increases the chance of data collision between tags which leads to deleterious performance in a large-scale deployment.

**Other Methods.** Besides methods mentioned above, there is an extensive body of RFID localization related studies. Liu *et al.* [34] introduces an hyperbolic localization method to associate the phase measurement with the target tag's location. Li *et al.* [35] leverages a multi-frequency based ranging method to locate the target tag. Tagoram [5] achieves a centimeter level tracking accuracy through the designed hologram which taking the thermal noise into consideration. Shangguan *et al.* [36] designs a tag ordering system by means of the spatial-temporal dynamics in the phase profiles. Further, a autonomous wheeled robot reader [7] is implemented achieves an exact spatial order in very close spacings. Although great progress has been made by these systems, effective RFID localization remains a great challenge to realize in a large-scale deployment.

**Large-scale Deployment.** Some of the recent works have attempted to address the problem of RFID localization in a large-scale deployment. The work presented in [1] introduces a novel location sensing system based on the geometric grid covering algorithm that can position or track objects inside buildings. This approach can successfully locate an object with an error of less than one meter. Reza *et al.* [37] propose a placement pattern of RFID reader antennas to maximize the reading coverage, delivering an average localization error of around 0.5 meter. Although these systems work well, they only work for a relatively smaller number of object tags. As a departure from the prior work, CSRP work effectively for a larger number of object tags with a smaller error, but requiring an order of magnitude fewer reference tags when compared with the state-of-the-art.

## VI. CONCLUSIONS

This paper has presented CSRP, a novel, fine-grained RFID positioning system based on compressive sensing. CSRP works on commercial RFID hardware, aiming to greatly reduce the number of reference tags required. CSRP utilizes the stable spatial relationship between the target object tag and reference tags to construct a noise-resilient fingerprint matrix. It then employs a compressive sensing based recovery algorithm to take in the fingerprint matrix and the real-time signal measurement to accurately localize the target item. We provide a set of analysis and methods for the optimal deployment of reference tags and for reducing the computational overhead of the localization algorithm. We evaluate CSRP by applying it to a real-world deployment of 255 commercial RFID tags. Experimental results show that CSRP can successfully locate 84.7% of the test items, reaching a performance-level that is comparable to the one provided by the state-of-the-art, but using only 9% of the reference tags required the state-of-the-art. This massive reduction in reference tags allows one to save significant deployment cost and time in a large-scale RFID deployment.

## ACKNOWLEDGEMENT

This work was supported in part by the UK Engineering and Physical Sciences Research Council under grants EP/M01567X/1 (SANDeRs) and EP/M015793/1 (DIVIDEND); and the Royal Society International Collaboration Grant (IE161012).

## REFERENCES

[1] L. M. Ni *et al.*, "LANDMARC: Indoor location sensing using active RFID," *Wireless Networks*, vol. 10, no. 6, pp. 701–710, 2004.
[2] J. Hightower *et al.*, "SpotON: An indoor 3D location sensing technology based on RF signal strength," *Uw Cse*, 2000.
[3] L. Shangguan *et al.*, "OTrack: Order tracking for luggage in mobile RFID systems," in *IEEE INFOCOM*, pp. 3066 – 3074, 2013.
[4] Y. Zhao *et al.*, "VIRE: Active RFID-based localization using virtual reference elimination," in *ICPP*, p. 56, 2007.
[5] L. Yang *et al.*, "Tagoram: real-time tracking of mobile RFID tags to high precision using COTS devices," in *ACM MobiCom*, pp. 237–248, 2014.
[6] J. Wang and D. Katabi, "Dude, where's my card?: RFID positioning that works with multipath and non-line of sight," in *ACM SIGCOMM Computer Communication Review*, vol. 43, pp. 51–62, 2013.
[7] L. Shangguan and K. Jamieson, "The design and implementation of a mobile RFID tag sorting robot," in *ACM MobiSys*, pp. 31–42, 2016.
[8] C. Hekimian-Williams *et al.*, "Accurate localization of RFID tags using phase difference," in *IEEE RFID*, pp. 89 – 96, 2010.
[9] P. V. Nikitin *et al.*, "Phase based spatial identification of UHF RFID tags," in *IEEE RFID*, pp. 102–109, 2010.
[10] S. Azzouzi *et al.*, "New measurement results for the localization of UHF RFID transponders using an angle of arrival (AoA) approach," in *IEEE RFID*, pp. 91–97, 2011.
[11] E. J. Candès and M. B. Wakin, "An introduction to compressive sampling," *IEEE Signal Processing Magazine*, vol. 25, no. 2, pp. 21–30, 2008.
[12] E. J. Candès *et al.*, "Stable signal recovery from incomplete and inaccurate measurements," *Communications on Pure & Applied Mathematics*, vol. 59, no. 8, pp. 1207–1223, 2006.
[13] J. Wang *et al.*, "E-HIPA: An Energy-Efficient framework for High-Precision Multi-Target adaptive Device-Free localization," *IEEE Trans. on Mobile Computing*, vol. 12, no. 5, pp. 1–12, 2016.
[14] D. Boufounos *et al.*, "A lecture on compressive sensing," *IEEE Signal Processing Magazine*, pp. 118–121, 2007.
[15] S. Salvador and P. Chan, "Toward accurate dynamic time warping in linear time and space," *Intelligent Data Analysis*, vol. 11, no. 5, pp. 561–580, 2007.
[16] K. Sheng *et al.*, "The collocation of measurement points in large open indoor environment," in *IEEE INFOCOM*, pp. 2488–2496, 2015.
[17] S. Yan *et al.*, "Graph embedding: A general framework for dimensionality reduction," in *IEEE CVPR*, vol. 2, pp. 830–837, 2005.
[18] D. L. Donoho *et al.*, "Sparse solution of underdetermined systems of linear equations by stagewise orthogonal matching pursuit," *IEEE Trans. on Information Theory*, vol. 58, no. 2, pp. 1094–1121, 2012.
[19] S. Si *et al.*, "Bregman divergence-based regularization for transfer subspace learning," *IEEE Trans. on Knowledge and Data Engineering*, vol. 22, no. 7, pp. 929–942, 2010.
[20] "Impinj, Inc." www.impinj.com/products/readers/speedway-revolution/.
[21] "Epc gen2, epcglobal." www.gs1.org/epcglobal.
[22] "Q900f-900 rfid antenna." www.hrtantenna.com/en/products.
[23] H. Ma and Y. Liu, "On coverage problems of directional sensor networks," in *International Conference on Mobile Ad-Hoc and Sensor Networks*, pp. 721–731, 2005.
[24] H. Ma, X. Zhang, and A. Ming, "A coverage-enhancing method for 3D directional sensor networks," in *INFOCOM*, pp. 2791–2795, 2009.
[25] S. Pradhan *et al.*, "RIO: A pervasive RFID-based touch gesture interface," in *The International Conference*, pp. 261–274, 2017.
[26] K. Lin *et al.*, "Enhanced fingerprinting and trajectory prediction for IoT localization in smart buildings," *IEEE Transactions on Automation Science Engineering*, vol. 13, no. 3, pp. 1294–1307, 2016.
[27] L. Yang *et al.*, "Frogeye: Perception of the slightest tag motion," in *IEEE INFOCOM*, pp. 2670–2678, 2014.
[28] J. D. Griffin and G. D. Durgin, "Complete link budgets for backscatter-radio and RFID systems," *IEEE Antennas and Propagation Magazine*, vol. 51, no. 2, pp. 11–25, 2009.
[29] J. Wang *et al.*, "RF-IDraw: virtual touch screen in the air using RF signals," in *ACM SIGCOMM Computer Communication Review*, vol. 44, pp. 235–246, 2014.
[30] A. Parr *et al.*, "Inverse sar approach for localization of moving RFID tags," in *IEEE RFID*, pp. 104–109, 2013.
[31] J. Wang *et al.*, "Rf-compass: Robot object manipulation using rfids," in *ACM MobiCom*, pp. 3–14, 2013.
[32] R. Miesen *et al.*, "Holographic localization of passive uhf rfid transponders," in *IEEE RFID*, pp. 32–37, 2011.
[33] A. Parr *et al.*, "A novel method for UHF RFID tag tracking based on acceleration data," in *IEEE RFID*, pp. 110–115, 2012.
[34] T. Liu *et al.*, "Anchor-free backscatter positioning for RFID tags with high accuracy," in *IEEE INFOCOM*, pp. 379 – 387, 2014.
[35] X. Li *et al.*, "Multifrequency-based range estimation of RFID tags," in *IEEE RFID*, pp. 147–154, 2009.
[36] L. Shangguan *et al.*, "Relative localization of rfid tags using spatial-temporal phase profiling," in *USENIX NSDI*, pp. 251–263, 2015.
[37] A. W. Reza and K. G. Tan, "Investigation of indoor location sensing via RFID reader network utilizing grid covering algorithm," *Wireless Personal Communications*, vol. 49, no. 1, pp. 67–80, 2009.